

Evaluation of Sentinel-2 and PlanetScope Image Fusion for Tree Species Identification in Wanagama Tropical Forest, Indonesia

Sarono.^{1*}, Muhammad Kamal.², Sigit Heru Murti BS.² and Emma Soraya.³

¹Doctoral Program in Geography, Faculty of Geography, Universitas Gadjah Mada,
Yogyakarta, Indonesia.

²Faculty of Geography, Universitas Gadjah Mada, Yogyakarta, Indonesia.

³Faculty of Forestry, Universitas Gadjah Mada, Yogyakarta, Indonesia.

[*sarono90@mail.ugm.ac.id](mailto:sarono90@mail.ugm.ac.id)

Abstract : Remote sensing-based tree species classification requires a combination of high spatial resolution and rich spectral information. Sentinel-2 offers advantages in spectral diversity and spectral consistency, but is limited by its spatial resolution of 10-20 meters. In contrast, PlanetScope provides finer spatial resolution (3.3 meters) and high revisit frequency, yet is often criticized for spectral inconsistency across satellites and potential radiometric noise. This study aims to evaluate the fusion of both sensors to improve species classification accuracy in the Wanagama Educational Forest, Gunung Kidul, Yogyakarta, by leveraging the spectral strength of Sentinel-2 and the spatial resolution of PlanetScope. Image fusion was carried out using the Gram-Schmidt method with two main schemes: (1) spectral band matching from Sentinel-2 pansharpened with first band (GS-PCA 1) of PCA extraction from PlanetScope RGB bands, and (2) second band (GS-PCA 2) of PCA extraction from PlanetScope RGB bands followed by pansharpening with Sentinel-2. Spectral validation was conducted using 700 random samples. The highest correlation was observed in the GS-PCA 1 approach ($R = 0.68$) against PlanetScope, also showed medium correlation with Sentinel 2 ($R = 0.33$), indicating that the generated fused data relates to both sources. Further classification was performed using 404 samples model and 151 ground truth with three parametric algorithms: Maximum Likelihood, Minimum Distance to Mean, and Mahalanobis Distance. The highest accuracy was achieved using GS-PCA 1 method under the Maximum Likelihood classifier, with an overall accuracy of 26.96%, outperforming Sentinel-2 (24.35%) and PlanetScope (23.48%). Although the accuracy remains moderate, this approach demonstrates the potential of multisensor fusion for tree species classification in tropical forests.

Keywords: Spectral Fusion, Sentinel-2, PlanetScope, Tree Species Classification, Gram-Schmidt PCA

1 Introduction

Tropical forests are among the world's most important ecosystems because they harbor high biodiversity, provide vital ecosystem services, and contribute substantially to regulating the global carbon cycle (Adhikari et al., 2024; ARKO, 2023). Understanding the distribution and composition of tree species is therefore essential to support conservation, forest governance, and biomass-to-carbon-stock assessment (Cook-Patton et al., 2020). However, high species richness, complex canopy architecture, and inherent spatial heterogeneity make tree-species classification in tropical forests a challenging scientific

problem (Food and Agriculture Organization of the United Nations, 1997; Kaimuddin et al., 2023). Remote sensing offers a practical way to overcome the limitations of conventional surveys. At the same time, the complexity of tree-species identification calls for integrating multiple sensors and analytical methods so that classifications become more accurate and scalable (Hussin, 2022; Xu et al., 2025).

Advances in remote sensing have created major opportunities to reduce the time and cost of field surveys in forestry and other domains (Hu et al., 2020). Today's optical satellites provide diverse spatial, spectral, and temporal resolutions, enabling more comprehensive descriptions of vegetation (DeRiggi, 2017). Sentinel-2 is widely used for vegetation monitoring because of its broad spectral coverage and strong radiometric consistency. Its red-edge, NIR, and SWIR bands, for example, have proven informative for species identification. Nevertheless, its 10–20 m spatial resolution is often insufficient to distinguish individual tree species (Xi et al., 2022, 2023). In contrast, PlanetScope offers ~3 m spatial resolution and near-daily revisit (Planet Labs, 2023), making it promising for frequent vegetation mapping (Purnamasari et al., 2021; Wang et al., 2023). Yet PlanetScope is often affected by inter-satellite radiometric variation and spectral inconsistency, which can degrade analysis quality (Basheer et al., 2024; Le et al., 2025).

These fundamental differences suggest complementary strengths and weaknesses. Multisensor fusion is therefore a promising strategy for tree-species analysis (Neyns et al., 2024, 2024). Through fusion, Sentinel-2's spectral richness can be combined with PlanetScope's spatial sharpness to produce more representative data. Gram–Schmidt pansharpening is a popular technique for this purpose because it enhances spatial detail while preserving spectral integrity (Leon et al., 2013; Maurer, 2013). Principal Component Analysis (PCA) can also be used to extract dominant information prior to fusion, improving the quality of the combined image (Centorame et al., 2025; Maciel Junior et al., 2024; Swain et al., 2024). Although satellite-data fusion has been explored for vegetation mapping, studies specifically evaluating Sentinel-2 and PlanetScope fusion for tree-species classification in tropical forests remain limited—despite the high biodiversity and conservation priority of these ecosystems (Herawati & Santoso, 2011; Njomaba et al., 2024).

This study focuses on the Wanagama Educational Forest, Gunung Kidul, Yogyakarta—an area with high tree-species diversity and an active outdoor laboratory (Ugm & H, 2019). We evaluate Sentinel-2 and PlanetScope fusion using the Gram–Schmidt (GS) method with two variants that use PC1 or PC2 from PlanetScope PCA as the synthetic panchromatic

input. We then assess spectral consistency, classify tree species using parametric algorithms, and compare the fused results against each sensor's native imagery. The study aims to provide a methodological contribution for multisensor fusion to improve tree-species classification accuracy in tropical forests and to support more effective, sustainable forest monitoring.

2 Literature Review

Multispectral optical sensors frequently used in forestry show that spectral richness—especially the red-edge, NIR, and SWIR—is critical for differentiating vegetation types (Assmann et al., 2019; Njomaba et al., 2024). However, classification accuracy tends to decline when the targets are sub-pixel, as in species-level analyses (Jain, 2022; Kluczek et al., 2023). Sentinel-2 is widely accessible and often used as a reference because of its mission design and excellent radiometric stability; its 10 m bands are commonly exploited for tree-species mapping and biophysical parameters such as LAI and chlorophyll. Prior work highlights the utility of Sentinel-2's red-edge, NIR, and SWIR bands for vegetation discrimination, with atmospheric correction and radiometric standardization crucial for temporal consistency (Persson et al., 2018; Xi et al., 2022). Still, the 10–20 m resolution often struggles to capture species variability in heterogeneous tropical canopies (Xi et al., 2023; Yu et al., 2022), underscoring the need to pair spectral strength with higher spatial detail.

Sentinel-2's spectral characteristics can reveal information hard to obtain from field surveys, such as plant physiological status, vegetation health, and subtle species differences despite similar morphology (Acharki, 2022; Finlayson et al., 2024). This underscores how spectral richness can detect small canopy variations not visible to the eye (Xie et al., 2008). However, limited spatial resolution remains a key barrier to separating closely packed objects in species-rich tropical ecosystems (Blickensdörfer et al., 2024). Mixed-pixel effects at medium resolution reduce mapping accuracy (T. Choe et al., 2025), where a single pixel may represent multiple land-cover types and blur species-specific spectral signals (Hemmerling et al., 2021; Mikołajczyk et al., 2025). Thus, while Sentinel-2 excels spectrally, its spatial detail shortfall requires complementary approaches (Bhattarai et al., 2021; Njimi et al., 2024).

PlanetScope shows a different profile (Aati et al., 2022; Baldin & Casella, 2024): its ~3 m spatial resolution and daily revisit enable richer object detail and temporal variability (Basheer et al., 2024; Labs, 2023; Neyns et al., 2024). The evolution to SuperDove increased spectral bands, though radiometric normalization demands more care (Niroumand-Jadidi et al., 2022; Silva et al., 2024). Quality evaluations reveal inter-satellite variation that must be resolved for multitemporal analysis (Chen et al., 2025; Hemingway & Frazier, 2021). In short, PlanetScope

provides strong spatial/temporal advantages but typically benefits from pairing with sensors that offer more stable spectral behavior (Mansaray et al., 2021).

Multisensor fusion studies consistently show that combining one sensor's strengths with another's can enhance remote-sensing analysis (Guo et al., 2024). Common goals include improving both spectral quality and spatial sharpness; radiometric normalization before/during fusion helps align sensors; and dimensionality reduction can simplify downstream analysis (Dhore & Veena, 2015). At the classification stage—whether using classic parametric algorithms or modern machine-learning methods—higher-resolution fused data often yields better accuracy (Chiang, 2014; Elbanby et al., 2012). Properly managed, Sentinel-2 + PlanetScope fusion can therefore boost tree-species classification, especially in complex tropical forests.

PCA has long been popular for multisensor fusion because it is simple and statistically grounded (Chiang, 2014; Elbanby et al., 2012). It can increase spatial contrast via high-resolution component injection, clarifying tree-crown structure and vegetation boundaries (H. P. Liu et al., 2025; Sule, 2020). However, PCA can be prone to spectral distortion when object spectral variability is complex—as in tropical forests (Tsai et al., 2007). Consequently, PCA is often combined with strict radiometric control or used as part of a broader fusion pipeline.

The Gram–Schmidt (GS) fusion method is widely applied because it improves spatial resolution while maintaining spectral consistency (Al-Doski et al., 2013). The process orthogonally transforms multispectral channels, replaces the first component with a (synthetic) panchromatic image, and then inverts the transform (Jovanović et al., 2016). GS tends to preserve critical spectral information—especially red and NIR bands crucial for vegetation and land-cover mapping (W.-I. Choe et al., 2024). In forestry, GS has been shown to improve tree-species classification by preserving ratios sensitive to biomass and canopy health (Vivone et al., 2015). In precision agriculture, GS supports more stable NDVI after fusion, improving stress detection and growth monitoring (Ghassemian, 2016; Rahmani et al., 2010). Performance remains sensitive to spectral mismatches and co-registration, so metrics such as ERGAS, SAM, and QNR are important for validation (Amro et al., 2011; Vivone et al., 2015). Fused products (via GS, PCA, or both) are commonly used as inputs for various classifiers—from classics like Maximum Likelihood (MLC) to machine-learning methods such as Random Forest (RF) and Support Vector Machine (SVM) (Binanto et al., 2024; Mateen et al., 2024; Zhang et al., 2025). Many studies report higher accuracies for species, land-cover, and biomass mapping with fusion compared to single-sensor data, often by 5–20% depending on ecosystem

complexity and inputs (Ghassemian, 2016; Vivone et al., 2015). For example, boreal forests have shown up to a 12% species-classification improvement after GS–PCA compared with original multispectral imagery (Rahmani et al., 2010). In tropical forests, combining fusion with vegetation indices (NDVI, EVI) and texture features can further separate species with similar canopy morphology, providing a richer basis for vegetation mapping (Mohammadpour & Viegas, 2022).

Fusion paired with deep learning has recently shown promising accuracy gains (Du et al., 2013). GS–PCA fused inputs combined with CNNs have, in some studies, improved tropical tree-species classification by >15% over conventional RF baselines (J. Liu et al., 2024), since CNNs can adaptively learn spatial–spectral patterns from fused imagery (Badidová et al., 2025). Thus, GS and PCA are not only image-quality enhancers but also strategic components in modern classification pipelines, with direct implications for species inventory, vegetation-health monitoring, and forest carbon-stock estimation in both boreal and tropical ecosystems (Ghassemian, 2016; J. Liu et al., 2024; Vivone et al., 2015)

3 Methodology

The study area is the Wanagama Forest, Gunung Kidul, Yogyakarta, Indonesia—a tropical forest featuring multiple tree species. As an educational forest, parts of the area are maintained as mixed plantings, while other plots are managed with deliberately planted species (Ugm & H, 2019). The official species map issued by the forest manager was used to derive training and test samples for classification. Two optical satellite datasets were employed with closely timed acquisitions: PlanetScope (~3.3 m; March 2025) and Sentinel-2 (10–20 m; April 2025), assumed to represent comparable on-ground conditions. The workflow (Figure 1) includes satellite corrections, derivation of a synthetic panchromatic band via PlanetScope PCA, Gram–Schmidt fusion, and subsequent analysis.

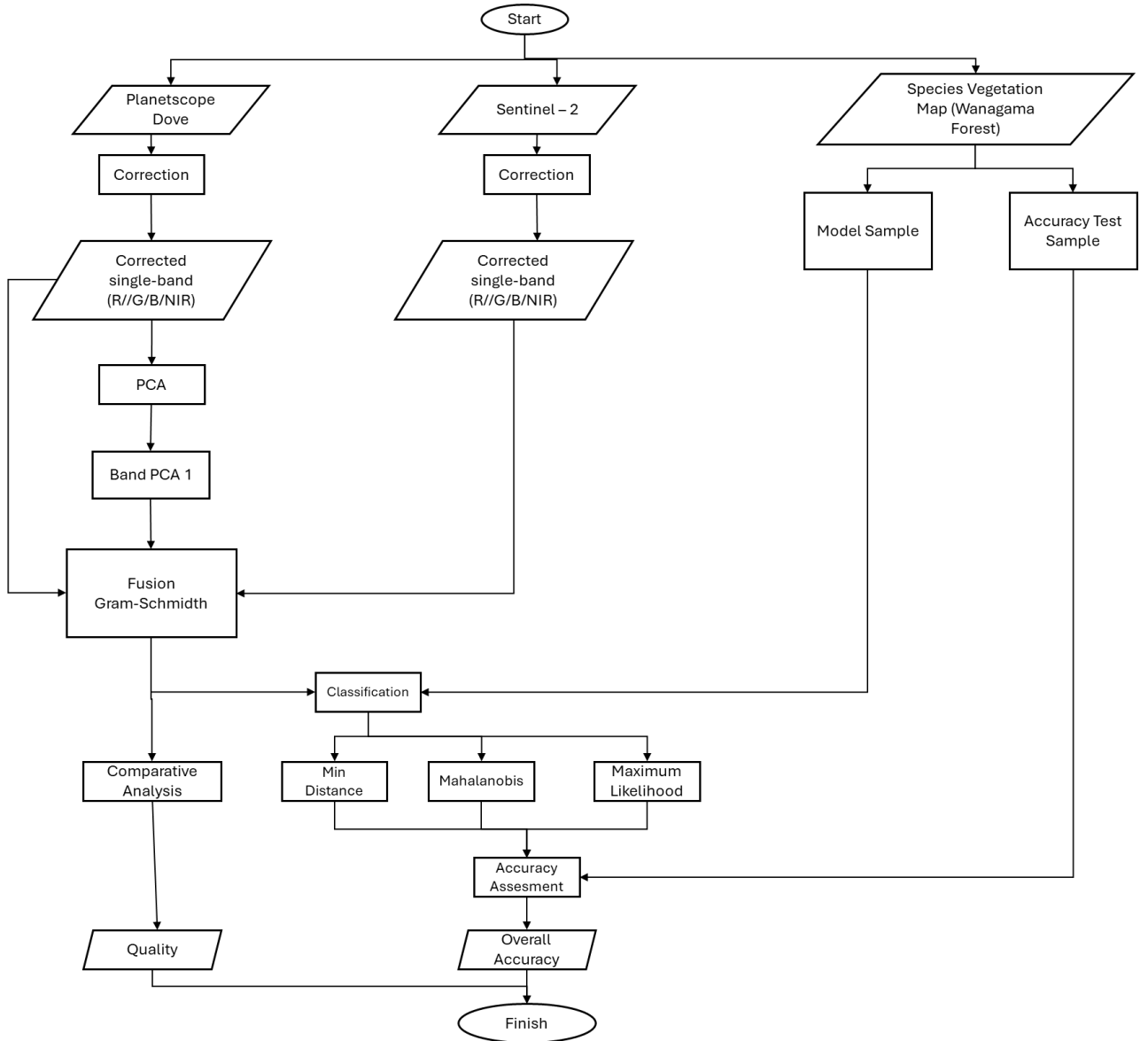


Figure 1: Methodology Diagram

a. Pre-processing data Satellite

In multi-sensor analyses, calibration is essential (Baldin & Casella, 2024; Basheer et al., 2024). We first performed radiometric correction to obtain surface reflectance for both PlanetScope (3.3 m) and Sentinel-2 (10–20 m). Conceptually, object reflectance ρ is derived from top-of-atmosphere radiance by removing atmospheric effects, ensuring that spectral values represent true surface conditions:

$$\rho = \frac{\pi \cdot L_{\lambda} \cdot d^2}{E_{sun} \cdot \cos\theta_s}$$

where λ is the spectral radiance, d is the relative Earth–Sun distance, E_{sun} is the solar irradiance, and θ_s is the solar zenith angle. This correction ensures that the analyzed spectral values represent the true spectral reflectance of objects on the Earth’s surface.

b. Training and Test Sample Design

Samples were selected using stratified random sampling based on the Wanagama species map. Stratification preserves proportionality across classes by area, avoiding classification bias (Keskintürk & Er, 2007; Sechidis et al., 2011). Data were split 70% for model training and 30% for independent testing, following supervised-classification best practices (Breiman, 2001; Kotsiantis et al., 2006; Mathur & Foody, 2008).

c. Synthetic Panchromatic Band Via PlanetScope SuperDove PCA

PlanetScope has four primary bands (R, G, B, NIR). We created a synthetic panchromatic band using PCA (Haque Shemul et al., 2022; Uddin et al., 2017). PCA reduces inter-band correlation via a linear transform; the first principal component (PC1) has the largest variance and is used as the panchromatic proxy (Chiang, 2014; Krishnan & Dutta, 2017). Secara matematis, PCA diturunkan dari dekomposisi kovarians:

$$Z = X.W$$

where X is a data matrix of size $n \times p$ (n samples, p bands), W is the eigenvector matrix of the covariance matrix, and Z is the result of the principal component transformation (Ghader et al., 2025). PC1 is used as the panchromatic channel because it contains the dominant spectral information (Dhanaraj & Markopoulos, 2019; Visentin et al., 2016).

d. PCA–Gram–Schmidt Image Fusion

In the first scheme (GS-PCA 1), PC1 from PlanetScope RGB PCA is used as the synthetic panchromatic input in Gram–Schmidt fusion with Sentinel-2. In the second scheme (GS-PCA 2), PC2 is used as the synthetic panchromatic source before GS fusion. This aims to combine PlanetScope’s spatial detail with Sentinel-2’s spectral consistency (Candra, 2013; Kuze & Sumantyo, 2010). Conceptually, the fused image F can be expressed as follows:

$$F = GS(MS, PC1)$$

where GS is the Gram–Schmidt operator, MS is the Sentinel-2 multispectral image, and $PC1$ is the first principal component derived from PlanetScope PCA (Maurer, 2013).

e. Linear Regression Analysis for Multispectral Bands Correlation

Linear regression analysis is used to evaluate spectral agreement by applying a simple linear regression between the fused image and the original Sentinel-2 or PlanetScope images. The relationship between bands is measured using the correlation coefficient (R^2):

$$y = a + bx + \epsilon$$

where y is the reflectance value of the fused image, x is the reflectance of the reference image, a is the intercept, b is the slope, and ε is the error (Forthofer et al., 2007). The coefficient of determination is calculated as:

$$R^2 = \frac{\sum(\hat{y} - \bar{y})^2}{\sum(y - \bar{y})^2}$$

An R^2 value approaching 1 indicates a strong spectral relationship between the fused image and the reference image (Cheng et al., 2014).

f. Tree-Species Classification

The classification stage was carried out using three parametric algorithms: Maximum Likelihood (ML), Minimum Distance to Mean (MDM), and Mahalanobis Distance (MD). The ML algorithm is based on probability theory with the assumption of a Gaussian distribution, so the probability of a pixel x belonging to class i can be expressed as:

$$P_i(x) = \frac{1}{(2\pi)^{d/2} |\Sigma_i|^{1/2}} \exp \left(-\frac{1}{2} (x - \mu_i)^T \Sigma_i^{-1} (x - \mu_i) \right)$$

where μ_i is the mean vector of class i , Σ_i is the covariance matrix, and d is the number of bands (Ghayour et al., 2021; Hogland et al., 2013). Pixels are classified into the class with the highest probability. The MDM and MD methods are distance-based variants, with MD accounting for correlations among bands through the covariance matrix (Kang & Katzfuss, 2023; Saboori et al., 2019).

g. Accuracy Assessment

Classification accuracy was evaluated using a confusion matrix comparing predicted classes with reference labels (Ahmad et al., 2012; BYJU's Classes, 2021). From this table, the overall accuracy value was calculated using the following formula:

Overall Accuracy (OA):

$$OA = \frac{\sum_i x_{ii}}{N}$$

where N is the total number of samples, x_{ii} is the number of correctly classified samples. A higher Kappa value indicates better classification reliability compared to relying solely on OA (Cai et al., 2018).

4 Results and Discussion

a. Fusion PCA-Gramschmidt

In the initial stage, a synthetic panchromatic band was generated using PCA applied to the PlanetScope RGB composite. The PCA extraction produced three new bands (PC1, PC2, and

PC3) representing spectral variations of the original image. As shown in Figure 2, PC1 and PC2 retained clear spatial information with good contrast and stable texture. In contrast, PC3 was dominated by noise, providing information that no longer accurately reflected surface conditions. This indicates that PC3 primarily captured disturbances or minor variance components without physical significance in the field.

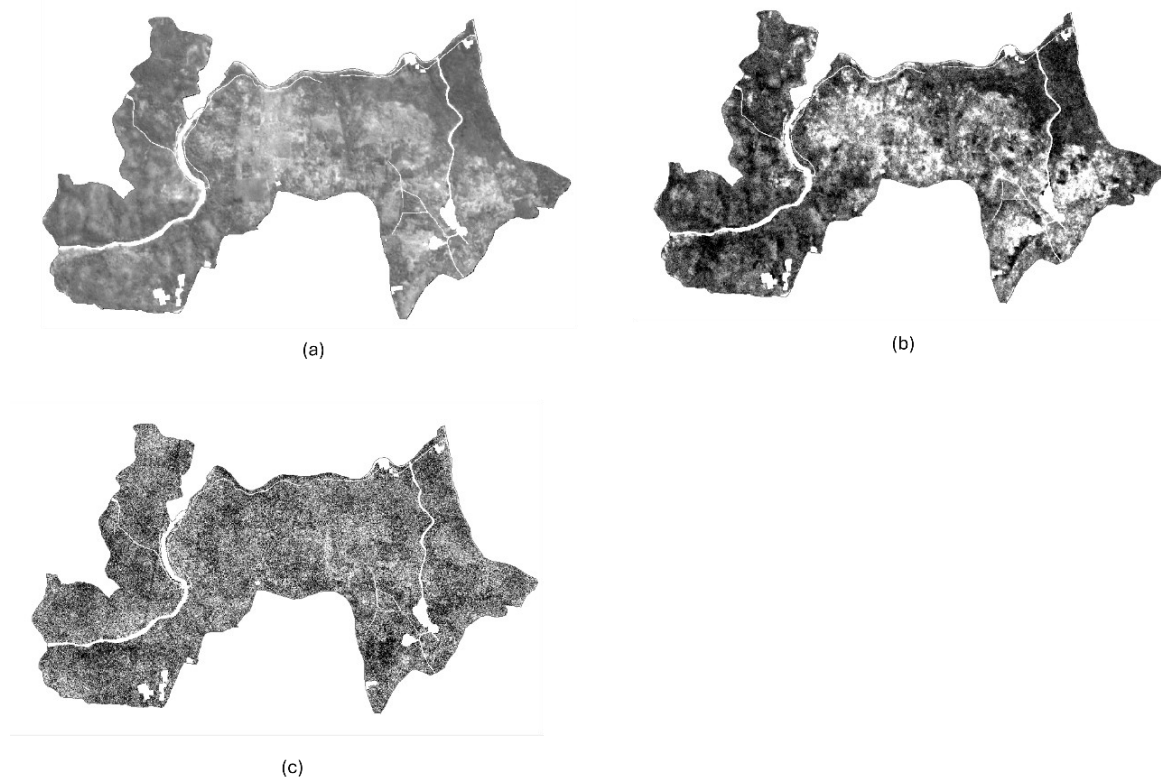


Figure 2: PCA Band of Visible Band PlanetScope

Based on these findings, only PC1 and PC2 were used to construct the synthetic panchromatic band, as they capture the largest proportion of variance from the original data and are more relevant for preserving spectral and spatial integrity. Excluding the noise-dominated PC3 made the analysis more stable, consistent, and suitable for subsequent fusion and classification. This highlights the importance of empirically evaluating PCA outputs to ensure that only components with strong physical meaning are applied in remote sensing analysis.

Fusion using the Gram–Schmidt method with PC1 showed clear differences compared to the input images. By injecting the high-resolution PC1 from PlanetScope into Sentinel-2, the fusion enhanced spatial sharpness. As illustrated in Figure 3, the fused image displayed finer canopy and vegetation structure detail than Sentinel-2 alone, while differing from PlanetScope due to the combined spectral characteristics of both satellites.

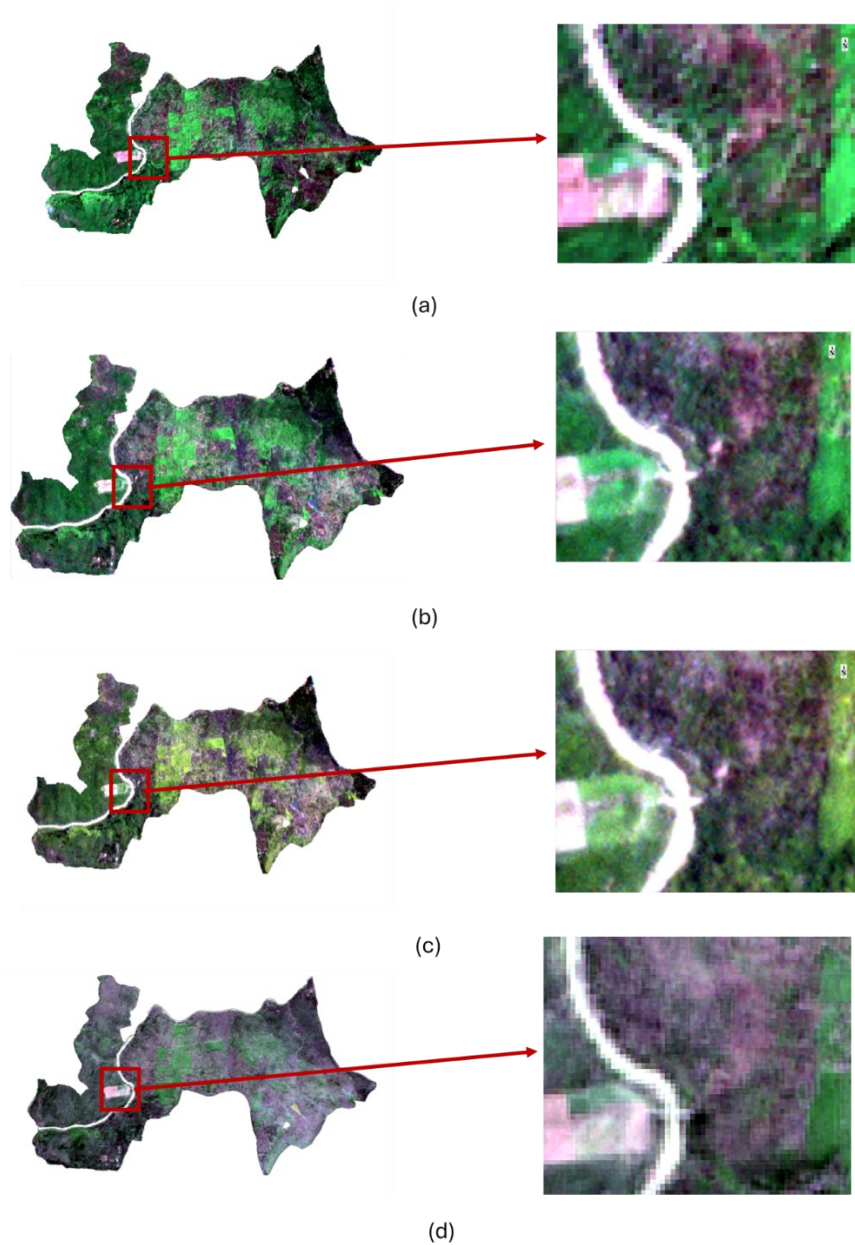


Figure 3: Sentinel-2 Imagery (a), PlanetScope Imagery (b), GS-PCA 1 Fusion Image (c), GS-PCA 2 Fusion Image (d)

From a spectral perspective, correlation analysis between the fused Sentinel-2 and PlanetScope images showed a visual resemblance closer to Sentinel-2, while adopting the finer spatial resolution of PlanetScope. This indicates that the method successfully preserved Sentinel-2's spectral characteristics even after transferring to higher spatial detail. As shown in Table 1, GS-PCA 1 generally outperformed GS-PCA 2, with correlation values closer to PlanetScope, reaching $r = 0.66$ – 0.71 for the RGB channels but lower in the NIR. In contrast, correlations with Sentinel-2 were highest in the NIR ($r \approx 0.54$). These results suggest that GS-PCA 1 is better suited for applications prioritizing spatial sharpness over full spectral consistency.

However, for vegetation classification that relies heavily on spectral richness, this approach still presents limitations.

Table 1: Correlation of GS-PCA Image fusion with original imagery

	GS PCA 1				GS PCA 2			
	Band Blue	Band Green	Band Red	Band NIR	Band Blue	Band Green	Band Red	Band NIR
PlanetScope	0,70	0,66	0,71	0,08	0,28	0,25	0,31	0,19
Sentinel 2	0,29	0,23	0,37	0,54	0,14	0,11	0,18	-0,12

Testing the spectral values of the GS-PCA 2 fusion showed correlations ranging from $r = 0.12$ – 0.31 , with the lowest in the NIR band and the highest in the Red band. Overall, the visible bands exhibited weaker correlations compared to GS-PCA 1. Figure 4 illustrates the linearity between GS-PCA 1 and Sentinel-2, where the highest R^2 appeared in the NIR band (0.28), while the visible bands were less representative. The low correlations are partly due to the large resolution gap between the synthetic panchromatic band (~ 3 m) and Sentinel-2 (10 m), about a 1:3 ratio, as well as spectral mismatches between the visible bands used for the panchromatic derivation and those of Sentinel-2. As shown in Figure 4, the NIR band achieved the strongest linearity, whereas the visible bands were more clustered and displayed weaker correlations.

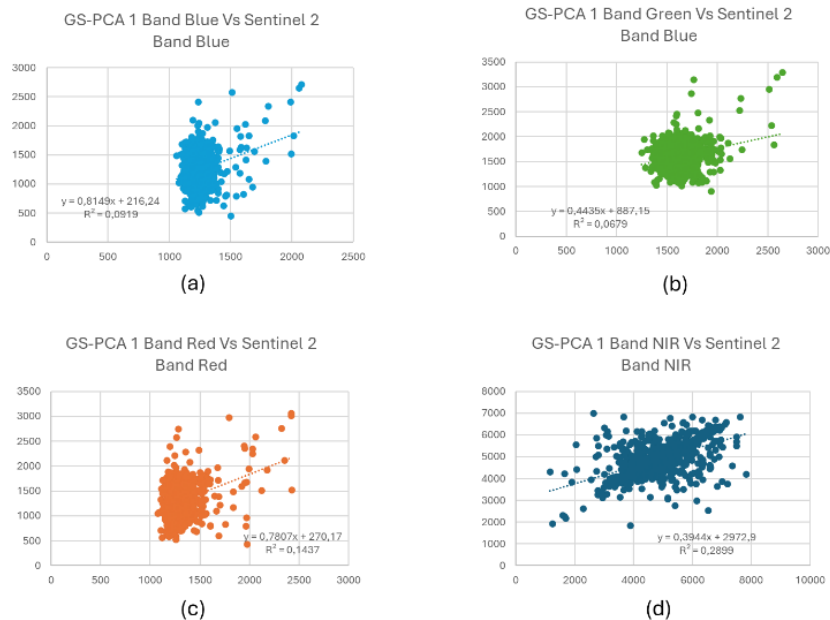


Figure 4: Comparative Fusion GS-PCA 1 VS Sentinel-2. Band Blue GS-PCA 1 Blue vs Blue Sentinel-2 (a), Band Green GS-PCA 1 Green vs Green Sentinel-2 (b), Band Red GS-PCA 1 Red vs Red Sentinel-2 (c), and Band NIR GS-PCA 1 NIR vs NIR Sentinel-2 (d)

The comparison of GS-PCA 1 fusion results with PlanetScope spectra showed better performance, as illustrated in Figure 5. The R^2 values ranged from 0.21 to 0.79, indicating stronger similarity to PlanetScope imagery. This suggests that the GS process effectively accounts for the spectral input while incorporating the higher spatial resolution, even though the fused spectral characteristics are influenced by the lower-resolution input. These findings highlight the importance of ensuring that the spectral ranges used for the synthetic panchromatic band are consistent or compatible with those of the other sensor in GS fusion, especially when combining data from different platforms.

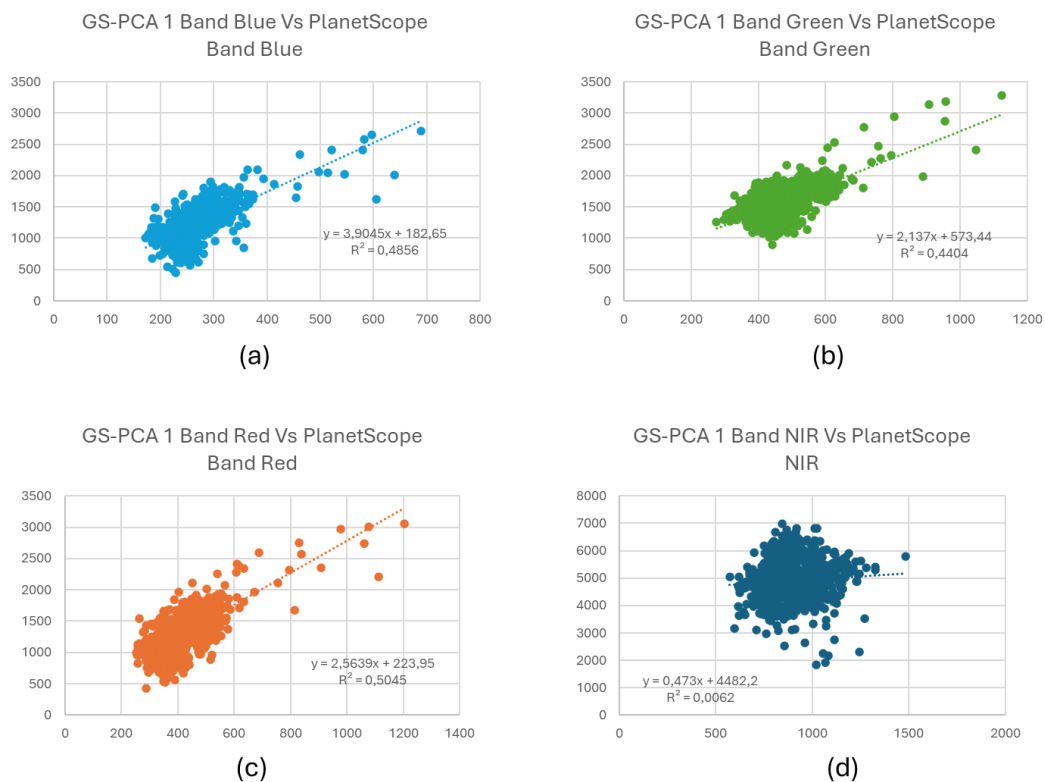


Figure 5: Comparative Fusion GS-PCA 1 VS PlanetScope, Band Blue GS-PCA 1 vs Blue PlanetScope (a), Band Green GS-PCA 1 vs Green PlanetScope (b), Band Red GS-PCA 1 vs Red PlanetScope (c), and Band NIR GS-PCA 1 vs NIR PlanetScope (d)

Compared to GS-PCA 1, the GS-PCA 2 method was processed using PC2 as the synthetic panchromatic input. As shown in Figure 6, the spectral similarity with Sentinel-2 was very low, with R^2 values ranging from 0.01 to 0.03—highest in the visible bands and lowest in the NIR. This confirms that most meaningful information is concentrated in PC1, while PC2 already loses significant detail and is dominated by noise. Therefore, PC1 is recommended for generating synthetic panchromatic bands with PCA, though further evaluation is needed. In the next stage, classification analysis will be carried out.

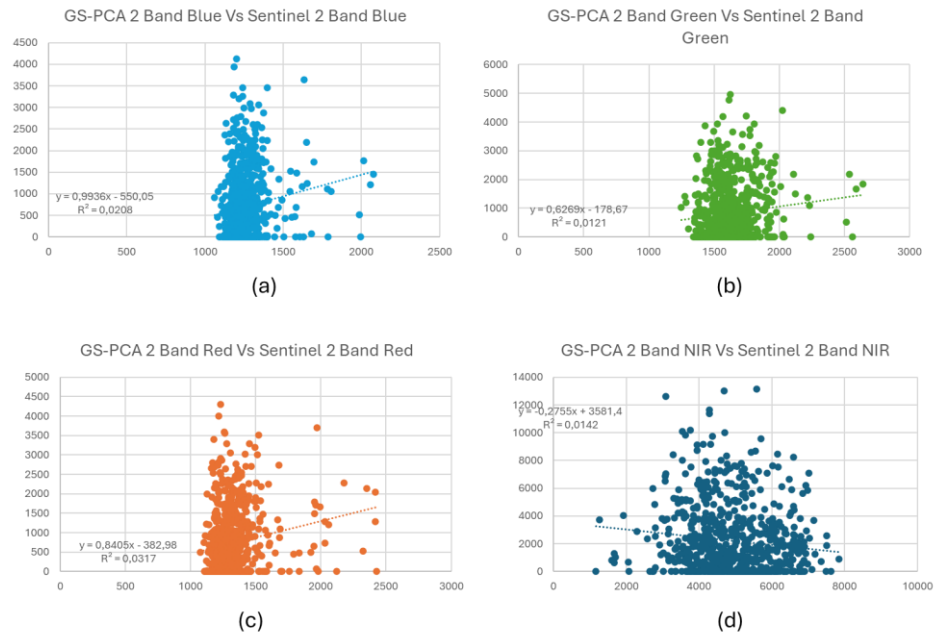


Figure 6: Comparative Fusion GS-PCA Band VS Sentinel-2. (a) Band Blue GS-PCA vs Blue Sentinel-2, (b) Band Green GS-PCA vs Green Sentinel-2, (c) Band Red GS-PCA vs Red Sentinel-2, (d) Band NIR GS-PCA vs NIR Sentinel-2

In contrast to the comparison with Sentinel-2, the GS-PCA 2 results showed low correlations with PlanetScope as well, with R^2 values of only 0.03–0.09 (Figure 7). Thus, GS-PCA 2 produced less reliable outcomes for both Sentinel-2 and PlanetScope, unlike GS-PCA 1, which at least showed a clear tendency toward PlanetScope characteristics.

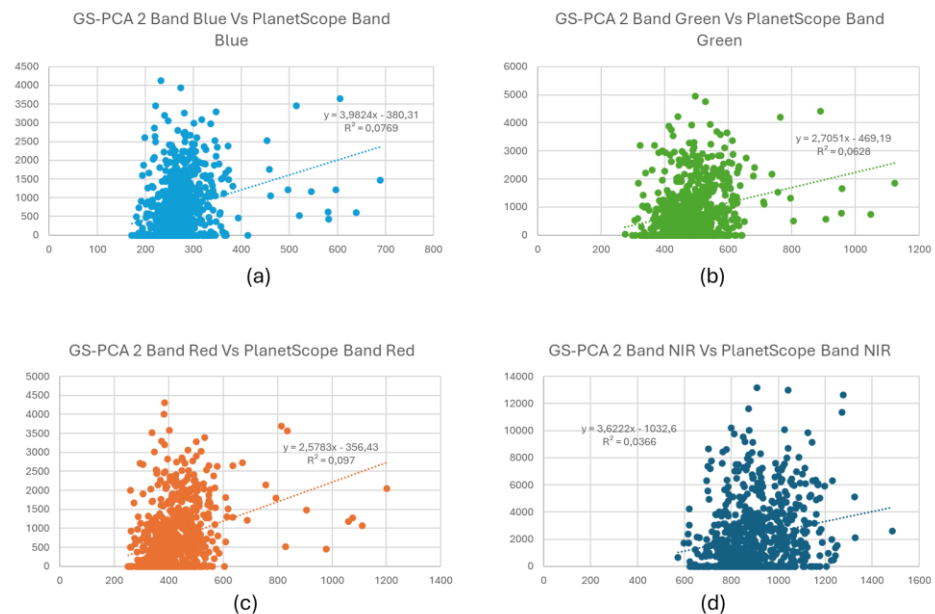


Figure 7: Comparative Fusion GS-PCA 2 vs PlanetScope, Band Blue GS-PCA 2 vs Blue PlanetScope (a), Band GS-PCA 2 vs Green PlanetScope (b), Band Red GS-PCA 2 vs Red PlanetScope (c), and Band NIR GS-PCA 2 vs NIR PlanetScope (d)

Thus, the GS-PCA 1 method can be regarded as the more appropriate approach for fusing the two images for species classification, as it preserves the spectral information needed to distinguish vegetation types while also providing high spatial detail useful for canopy identification. Based on these findings, the classification evaluation was conducted on GS-PCA 1 to assess its performance.

b. Minimum Distance to Mean (MDM) Classification

Classification using the MDM algorithm produced relatively simple yet stable performance based on the input satellite data. This algorithm calculates the Euclidean distance between each test pixel and the class centroids, assigning the pixel to the class with the smallest distance. The results showed that MDM tends to be accurate for classes with homogeneous spectral distributions. As seen in Figure 8, *Gliricidia* appeared in nearly the same locations across all three maps, but under GS-PCA 1 the species mahogany, teak, and *Gliricidia* were classified more clearly than in the other datasets. This limitation arises because MDM does not account for inter-band covariance, making it vulnerable to overlaps among complex classes.

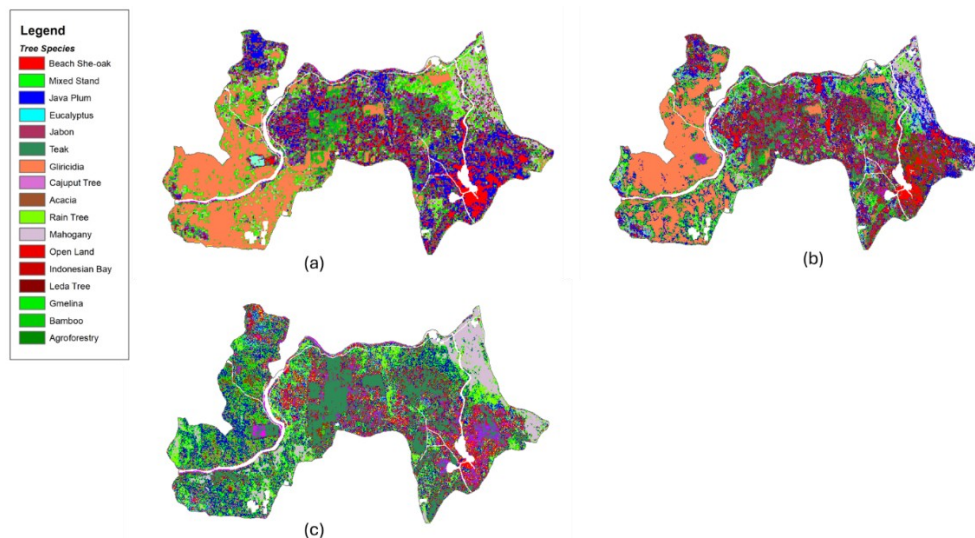


Figure 8: MDM Classification Result, Sentinel-2 (a), PlanetScope (b), and GS-PCA 1 (c)

The fusion results of the two images showed that GS-PCA 1 generally produced patterns resembling both Sentinel-2 and PlanetScope, particularly for the *Gliricidia* species, which appeared in similar locations marked in orange. This confirms that GS-PCA fusion offers a better compromise between the spectral consistency of Sentinel-2 and the spatial sharpness of PlanetScope, although the classification accuracy under MDM remains moderate due to the limitations of a purely Euclidean distance-based method.

c. Mahalanobis Distance (MD) Classification

Classification with the Mahalanobis Distance (MD) algorithm provided more adaptive results compared to MDM, as it considers the covariance structure between spectral bands. This allows the method to better handle classes with overlapping spectral ranges. In Figure 9, the GS-PCA 1 results demonstrated clearer separations for species such as mahogany, teak, and Gliricidia, which appeared more scattered under PlanetScope and Sentinel-2 alone. However, the method requires sufficient and representative training samples to avoid biased covariance estimates.

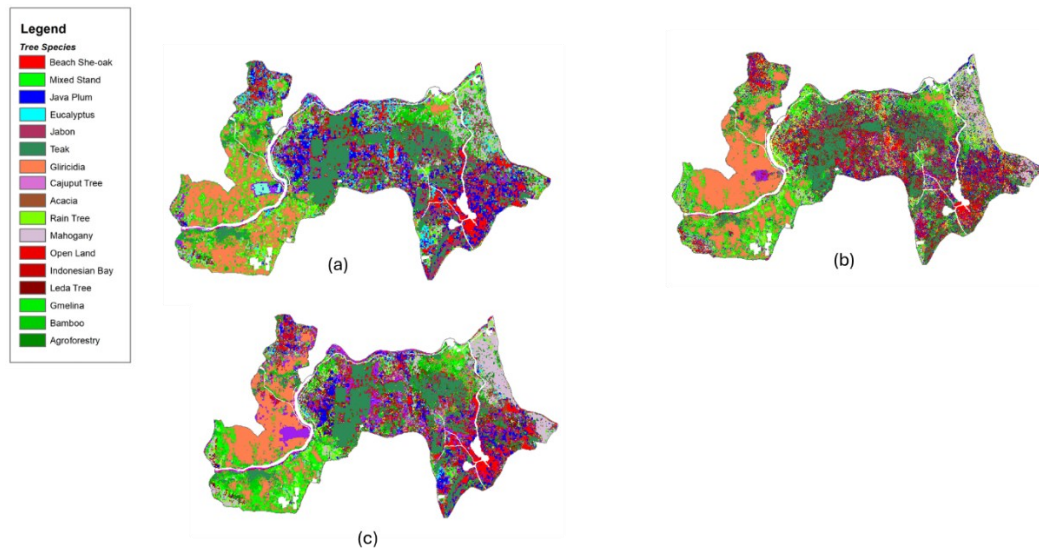


Figure 9: Mahalanobis Classification , Sentinel-2 (a), PlanetScope (b), and GS-PCA 1 (c) When sample numbers are limited, class boundaries may become unstable, leading to moderate accuracy. Nonetheless, the MD algorithm highlighted the potential of GS-PCA 1 fusion to improve discrimination in heterogeneous forest stands.

d. Maximum Likelihood (ML) Classification

The Maximum Likelihood (ML) method is a classical algorithm widely applied in remote sensing. ML assumes a Gaussian distribution for each class and calculates the membership probability of each pixel, assigning it to the class with the highest probability. The results indicated that ML is highly effective for classes with distributions close to normal, generally producing higher accuracy than MDM. In Wanagama Forest, ML captured spectral variation among species, although some classes with complex spectral distributions remained difficult to separate. As shown in *Figure 10*, the GS-PCA 1 fusion successfully identified teak, mahogany, and Gliricidia as distinct, well-clustered classes. This demonstrates that ML's statistical framework is well suited for classifying dominant vegetation species over larger areas, and that GS-PCA 1 fusion provides the spatial-spectral conditions to support such classification effectively.

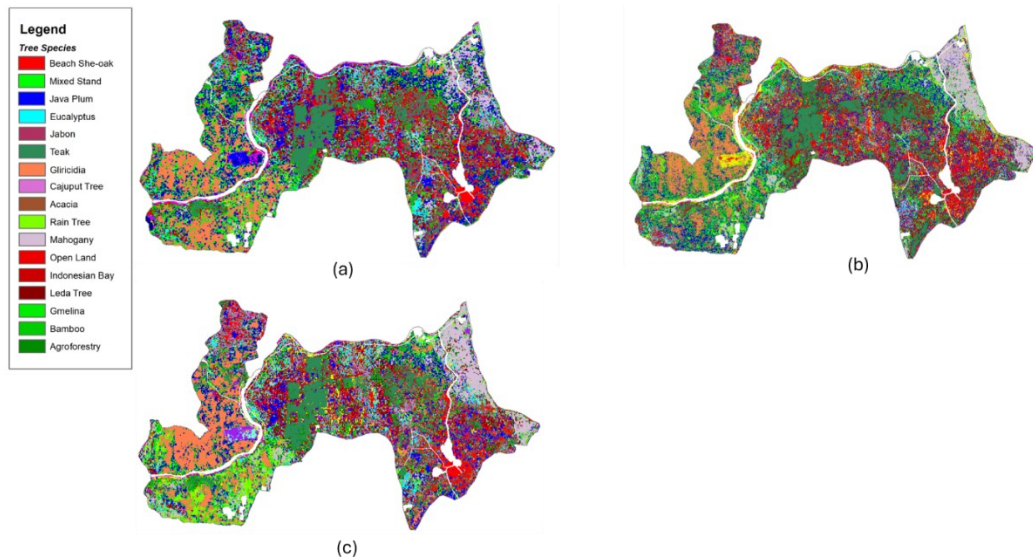


Figure 10. ML Classification, such as Sentinel-2 (a), PlanetCope (b), and GS-PCA 1 (c) As a probabilistic algorithm, ML offers advantages in statistical interpretation. However, its sensitivity to the size and representativeness of training data remains a challenge. When training samples do not adequately capture class distributions, the computed probabilities may become biased, reducing overall accuracy. This can be observed in Figure 11, where mixed or non-dominant objects appear scattered and inconsistencies arise between Sentinel-2, PlanetScope, and both GS-PCA results. Figure 11 below presents the map with the highest accuracy, obtained from the GS-PCA 1 fusion processed with the ML method..

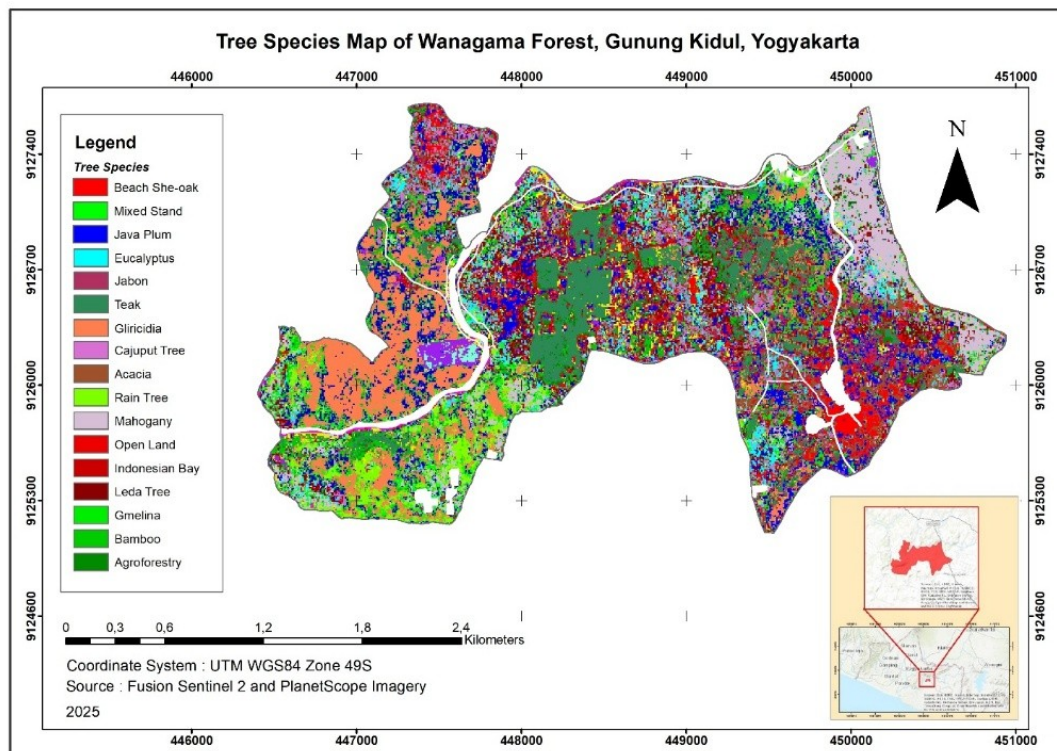


Figure 11. Map of Tree Species in Wanagama Forest with Maximum Likelihood

e. Accuracy Test

Accuracy evaluation in this study focused on Overall Accuracy (OA), which represents the proportion of correctly classified samples relative to the total test set. The results showed that the Maximum Likelihood method achieved the highest OA with the GS-PCA 1 combination (26.96%), slightly outperforming single-sensor Planet (23.48%) and Sentinel-2 (24.35%). Under the Minimum Distance method, accuracy was higher for Planet (17.39%) and GS-PCA 2 (16.52%), while GS-PCA 1 decreased to 9.57%.

Table 2. Table of Tree Species Classification Accuracy

Imagery	Number of Band	Sum	Count	Overall Accuracy
Maximumlikelihood				
Planet	4 band	27	115	23,48%
Sentinel 2	4 band	28	115	24,35%
GS-PCA 1	4 band	31	115	26,96%
Minimum Distance				
Planet	4 band	20	115	17,39%
Sentinel 2	4 band	12	115	10,43%
GS-PCA 1	4 band	11	115	9,57%
Mahalanobis				
Planet	4 band	29	115	25,22%
Sentinel 2	4 band	25	115	21,74%
GS-PCA 1	4 band	26	115	22,61%

Overall, the Mahalanobis method also showed a relatively good trend, with the highest OA obtained from Planet (25.22%) and GS-PCA 1 (22.61%). This pattern indicates that GS-PCA fusion provides higher accuracy than single-sensor Sentinel-2, although the improvement is not substantial. These findings suggest that the combined contribution of spatial resolution and spectral richness from the multisensor approach remains valuable for improving classification accuracy, even if the gains are still moderate.

f. Discussion

This study highlights both the potential and limitations of multisensor image fusion for tree species classification in tropical forests. In general, fusion improves spatial detail while retaining spectral information, but classification accuracy remains moderate, requiring further development. A key limitation is the spectral resolution of PlanetScope, which has only four

bands compared to Sentinel-2's thirteen. While fusion enhances spatial sharpness, the complex spectral variability of tropical vegetation remains difficult to capture fully. Moreover, the choice of classification algorithm strongly influences outcomes. Classical parametric methods such as ML provided some improvements, but the gains were not substantial. Future research should therefore explore machine learning and deep learning approaches to achieve higher classification accuracy in tropical forests.

This approach proved capable of producing tree species classification maps, though the achieved accuracy is still not ideal. The complexity of tropical forests, with their high species diversity, leads to overlapping spectra between classes, making it difficult to separate species using only medium-resolution multisensor combinations. Accuracy limitations also stem from the reference data employed: in this study, ground-based thematic maps were used as the sampling basis. While valid, such data lack the spatial detail of very high-resolution aerial surveys, which offer a higher measurement hierarchy and lower classification error.

The fusion of Sentinel-2 and PlanetScope can thus be considered a viable alternative for medium-scale species classification. However, given that the accuracy remains moderate despite higher spatial resolution, the results should be regarded as exploratory. To improve accuracy, future studies should integrate more detailed field data, high-resolution aerial imagery, or even LiDAR, which provides three-dimensional canopy structure, thereby enabling species classification in tropical forests with greater precision and closer to real conditions.

5 Conclusion and Recommendation

The results show that multisensor fusion between Sentinel-2 and PlanetScope can improve accuracy in tree species classification. The GS-PCA 1 approach produced moderate correlations with Sentinel-2 spectra and higher correlations with PlanetScope, while GS-PCA 2 displayed weaker correlations with both. This indicates that the fused data were able to preserve relationships with both sensors in terms of spectral and spatial characteristics. Classification of the GS-PCA 1 fused image using the Maximum Likelihood algorithm achieved the highest accuracy (26.96%), surpassing single-sensor Sentinel-2 (24.35%) and PlanetScope (23.48%). Although the improvement remains moderate, these results provide empirical evidence that multisensor integration can mitigate the limitations of individual satellites. Thus, this study demonstrates that combining the spectral strength of Sentinel-2 with the spatial sharpness of PlanetScope holds real potential for supporting tree species classification in tropical forests.

a. Recommendation

The findings highlight the need to test fusion methods using PCA inputs from a broader range of satellite imagery, such as Landsat, SPOT, PlanetScope, and Pleiades, beyond the Sentinel-2 and PlanetScope combinations. Integrating multisensor data with diverse spectral and spatial characteristics can enrich information and improve the stability of fusion results. This approach allows the performance of Gram-Schmidt and PCA methods to be evaluated more comprehensively across different sensor contexts.

In addition, high-resolution multispectral aerial imagery can serve as valuable reference data to strengthen validation, reducing reliance solely on satellite sources. Future studies are recommended to begin with fewer species to minimize classification complexity, while independently collecting field data to ensure quality and representativeness. PCA band selection should holistically consider variance, inter-band correlation, and relevance to biophysical parameters, thereby improving species classification accuracy in tropical forests.

References

- Aati, S., Avouac, J.-P., Rupnik, E., & Pierrot-Deseilligny, M.-P. (2022). Potential and Limitation of PlanetScope Images for 2-D and 3-D Earth Surface Monitoring With Example of Applications to Glaciers and Earthquakes. *IEEE Transactions on Geoscience and Remote Sensing*, 60. Scopus. <https://doi.org/10.1109/TGRS.2022.3215821>
- Acharki, S. (2022). PlanetScope contributions compared to Sentinel-2, and Landsat-8 for LULC mapping. *Remote Sensing Applications: Society and Environment*, 27. Scopus. <https://doi.org/10.1016/j.rsase.2022.100774>
- Adhikari, D., Singh, P. P., Tiwary, R., & Barik, S. K. (2024). Forest carbon stock-based bioeconomy: Mixed models improve accuracy of tree biomass estimates. *Biomass and Bioenergy*, 183, 107142–107142. <https://doi.org/10.1016/j.biombioe.2024.107142>
- Ahmad, A., Leh, L. C., & Udin, W. S. (2012). Accuracy assessment of aerial triangulation using different format of aerial photograph and digital photogrammetric software. *Proceedings - 2012 IEEE 8th International Colloquium on Signal Processing and Its Applications, CSPA 2012*, 413–418. <https://doi.org/10.1109/CSPA.2012.6194760>
- Al-Doski, J., Mansorl, S. B., & Shafri, H. Z. M. (2013). Image classification in remote sensing. *Department of Civil Engineering, Faculty of Engineering, University Putra, Malaysia*, 3(10).
- Amro, I., Mateos, J., Vega, M., Molina, R., & Katsaggelos, A. K. (2011). A survey of classical methods and new trends in pansharpening of multispectral images. *EURASIP Journal on Advances in Signal Processing*, 2011(1), 79. <https://doi.org/10.1186/1687-6180-2011-79>
- ARKO. (2023, May 29). *Role of Forestry Law in Combating Climate Change*. <https://armilarako.com/insights/forestry-law-combating-climate-change>
- Assmann, J. J., Kerby, J. T., Cunliffe, A. M., & Myers-Smith, I. H. (2019). Vegetation monitoring using multispectral sensors—Best practices and lessons learned from high latitudes. *Journal of Unmanned Vehicle Systems*, 7(1), 54–75. <https://doi.org/10.1139/juvs-2018-0018>
- Badidová, B., Forgáč, R., Očkay, M., Javurek, M., Krammer, P., & Hluchý, L. (2025). A Dual-Camera Analysis of PCA Coefficients for Hyperspectral Classification of Tree Species. *2025 Cybernetics & Informatics (K&I)*, 1–5. <https://doi.org/10.1109/KI64036.2025.10916439>
- Baldin, C. M., & Casella, V. M. (2024). Vegetative Index Intercalibration Between PlanetScope and Sentinel-2 Through a SkySat Classification in the Context of “Riserva San Massimo” Rice Farm in Northern Italy. *Remote Sensing*, 16(21). Scopus. <https://doi.org/10.3390/rs16213921>
- Basheer, S., Wang, X., Nawaz, R. A., Pang, T., Adekanmbi, T., & Mahmood, M. Q. (2024). A comparative analysis of PlanetScope 4-band and 8-band imageries for land use land cover classification. *Geomatica*, 76(2). Scopus. <https://doi.org/10.1016/j.geomat.2024.100023>
- Bhattarai, R., Rahimzadeh-Bajgiran, P., Weiskittel, A., Meneghini, A., & MacLean, D. A. (2021). Spruce budworm tree host species distribution and abundance mapping using multi-temporal Sentinel-1 and Sentinel-2 satellite imagery. *ISPRS Journal of Photogrammetry and Remote Sensing*, 172, 28–40. Scopus. <https://doi.org/10.1016/j.isprsjprs.2020.11.023>
- Binanto, I., Devina Ayuningtyas, B. M., & Sianipar, N. F. (2024). The Effect of Data Balancing on Performance of Support Vector Machine and Random Forest Classification for Typhonium Flagelliforme Lodd Dataset. *2024 International*

- Conference on Informatics Electrical and Electronics (ICIEE)*, 1–3.
<https://doi.org/10.1109/ICIEE63403.2024.10920451>
- Blickensdörfer, L., Oehmichen, K., Pflugmacher, D., Kleinschmit, B., & Hostert, P. (2024). National tree species mapping using Sentinel-1/2 time series and German National Forest Inventory data. *Remote Sensing of Environment*, 304, 114069.
<https://doi.org/10.1016/j.rse.2024.114069>
- Breiman, L. (2001). Random forests. *Machine Learning*, 45, 5–32.
- BYJU's Classes. (2021). *Accuracy and Precision—The Art of Measurement*.
<https://byjus.com/physics/accuracy-precision-measurement/>
- Cai, L., Shi, W., Miao, Z., & Hao, M. (2018). Accuracy assessment measures for object extraction from remote sensing images. *Remote Sensing*, 10(2).
<https://doi.org/10.3390/rs10020303>
- Candra, D. S. (2013). *Analysis of SPOT-6 data fusion using Gram-Schmidt spectral sharpening on agriculture land*. 1, 839–844. Scopus.
<https://www.scopus.com/inward/record.uri?eid=2-s2.0-84903486787&partnerID=40&md5=50f9eede01877baabbc11f353b33f464>
- Centorame, L., La Porta, N., Papandrea, M., Mancini, A., & Foppa Pedretti, E. (2025). Evaluation of Feature Selection and Regression Models to Predict Biomass of Sweet Basil by Using Drone and Satellite Imagery. *Applied Sciences (Switzerland)*, 15(11). Scopus. <https://doi.org/10.3390/app15116227>
- Chen, R., Yang, W., Chen, X., Gu, Z., Yin, B., Zhang, Y., & Chen, J. (2025). Harmoni-Planet: A holistic harmonization method for PlanetScope constellation imagery leveraging a graph-based greedy optimization strategy. *Remote Sensing of Environment*, 330, 114986. <https://doi.org/10.1016/j.rse.2025.114986>
- Cheng, C.-L., Shalabh, & Garg, G. (2014). Coefficient of determination for multiple measurement error models. *Journal of Multivariate Analysis*, 126, 137–152.
<https://doi.org/10.1016/j.jmva.2014.01.006>
- Chiang, J.-L. (2014). Knowledge-based Principal Component Analysis for Image Fusion. *Applied Mathematics & Information Sciences*, 8(1L), 223–230.
<https://doi.org/10.12785/amis/081L28>
- Choe, T., Jeon, S., Kim, B., & Park, S. (2025). From Coarse to Crisp: Enhancing Tree Species Maps with Deep Learning and Satellite Imagery. *Remote Sensing*, 17(13), 2222. <https://doi.org/10.3390/rs17132222>
- Choe, W.-I., Jo, J.-S., Ri, K.-S., Sok, K.-C., & Ri, Y.-R. (2024). Improving Gram–Schmidt Adaptive Pansharpening Method Using Support Vector Regression and Markov Random Field. *Journal of the Indian Society of Remote Sensing*, 52(9), 2073–2081.
<https://doi.org/10.1007/s12524-024-01934-x>
- Cook-Patton, S. C., Leavitt, S. M., Gibbs, D., Harris, N. L., Lister, K., Anderson-Teixeira, K. J., Briggs, R. D., Chazdon, R. L., Crowther, T. W., Ellis, P. W., Griscom, H. P., Herrmann, V., Holl, K. D., Houghton, R. A., Larrosa, C., Lomax, G., Lucas, R., Madsen, P., Malhi, Y., ... Griscom, B. W. (2020). Mapping carbon accumulation potential from global natural forest regrowth. *Nature*, 585(7826), 545–550.
<https://doi.org/10.1038/s41586-020-2686-x>
- DeRiggi, J. (2017). *Remote Sensing Part 3: Identify Healthy Vegetation from Space*.
<https://dai-global-digital.com/lush-green-remote-sensing.html>
- Dhanaraj, M., & Markopoulos, P. P. (2019). Stochastic Principal Component Analysis Via Mean Absolute Projection Maximization. *2019 IEEE Global Conference on Signal and Information Processing (GlobalSIP)*, 1–5.
<https://doi.org/10.1109/GlobalSIP45357.2019.8969411>

- Dhore, A. D., & Veena, C. S. (2015). Evaluation of various pansharpening methods using image quality metrics. *2015 2nd International Conference on Electronics and Communication Systems (ICECS)*, 871–877. <https://doi.org/10.1109/ECS.2015.7125039>
- Du, P., Chen, Y., Xia, J., & Tan, K. (2013). A Novel Remote Sensing Image Classification Scheme Based on Data Fusion, Multiple Features and Ensemble Learning. *Journal of the Indian Society of Remote Sensing*, 41(2), 213–222. <https://doi.org/10.1007/s12524-012-0205-8>
- Elbanby, G., Madbouly, E. E., & Abdalla, A. (2012). Fuzzy principal component analysis for sensor fusion. *2012 11th International Conference on Information Science, Signal Processing and Their Applications (ISSPA)*, 442–447. <https://doi.org/10.1109/ISSPA.2012.6310591>
- Finlayson, C., Hethcoat, M. G., Cannon, P. G., Bryant, R. G., Yusah, K. M., Edwards, D. P., & Freckleton, R. P. (2024). Monitoring lianas from space: Using Sentinel-2 imagery to observe liana removal in logged tropical forests. *Forest Ecology and Management*, 554, 121648. <https://doi.org/10.1016/j.foreco.2023.121648>
- Food and Agriculture Organization of the United Nations. (1997). *Basic wood densities of tropical tree species*. FAO. <https://www.fao.org/3/j2132s/j2132s17.htm>
- Forthofer, R. N., Lee, E. S., & Hernandez, M. (2007). Linear Regression. In *Biostatistics* (pp. 349–386). Elsevier. <https://doi.org/10.1016/B978-0-12-369492-8.50018-2>
- Ghader, M., Abdolmaleki, M., & Dana Mazraeh, H. (2025). Principal and independent component analysis methods. In *Dimensionality Reduction in Machine Learning* (pp. 65–107). Elsevier. <https://doi.org/10.1016/B978-0-44-332818-3.00012-5>
- Ghassemian, H. (2016). A review of remote sensing image fusion methods. *Information Fusion*, 32, 75–89. <https://doi.org/10.1016/j.inffus.2016.03.003>
- Ghayour, L., Neshat, A., Paryani, S., Shahabi, H., Shirzadi, A., Chen, W., Al-Ansari, N., Geertsema, M., Pourmehdi Amiri, M., Gholamnia, M., Dou, J., & Ahmad, A. (2021). Performance Evaluation of Sentinel-2 and Landsat 8 OLI Data for Land Cover/Use Classification Using a Comparison between Machine Learning Algorithms. *Remote Sensing*, 13(7), 1349. <https://doi.org/10.3390/rs13071349>
- Guo, Y., Wang, N., Wei, X., Zhou, M., Wang, H., & Bai, Y. (2024). Desert oasis vegetation information extraction by PLANET and unmanned aerial vehicle image fusion. *Ecological Indicators*, 166, 112516–112516. <https://doi.org/10.1016/j.ecolind.2024.112516>
- Haque Shemul, Md. S., Rahman, M. M., Ahmed, S., Marjan, Md. A., Uddin, Md. P., & Afjal, M. I. (2022). Segmented-Sparse-PCA for Hyperspectral Image Classification. *2022 4th International Conference on Electrical, Computer & Telecommunication Engineering (ICECTE)*, 167–170. <https://doi.org/10.1109/ICECTE57896.2022.10114537>
- Hemingway, B. L., & Frazier, A. E. (2021). Cross-sensor radiometric normalization of Planet smallsat data using Sentinel-2 to improve consistency across scenes and environments. In L. Bruzzone, F. Bovolo, & J. A. Benediktsson (Eds.), *Image and Signal Processing for Remote Sensing XXVII* (p. 1). SPIE. <https://doi.org/10.1117/12.2600246>
- Hemmerling, J., Pflugmacher, D., & Hostert, P. (2021). Mapping temperate forest tree species using dense Sentinel-2 time series. *Remote Sensing of Environment*, 267, 112743. <https://doi.org/10.1016/j.rse.2021.112743>
- Herawati, H., & Santoso, H. (2011). Tropical forest susceptibility to and risk of fire under changing climate: A review of fire nature, policy and institutions in Indonesia. *Forest Policy and Economics*, 13(4), 227–233. <https://doi.org/10.1016/j.forpol.2011.02.006>

- Hogland, J., Billor, N., & Anderson, N. (2013). Comparison of standard maximum likelihood classification and polytomous logistic regression used in remote sensing. *European Journal of Remote Sensing*, 46(1), 623–640. <https://doi.org/10.5721/EuJRS20134637>
- Hu, T., Sun, X., Su, Y., Guan, H., Sun, Q., Kelly, M., & Guo, Q. (2020). Development and Performance Evaluation of a Very Low-Cost UAV-Lidar System for Forestry Applications. *Remote Sensing*, 13(1), 77–77. <https://doi.org/10.3390/rs13010077>
- Hussin, Y. A. (2022). Assessment and Modelling of Forest Biomass and Carbon Stock and Sequestration Using Various Remote Sensing Sensor Systems. In *Concepts and Applications of Remote Sensing in Forestry* (pp. 75–95). Springer Nature Singapore.
- Jain, H. (2022). *Tree species classification based on machine learning techniques: Mapping Chir pine in Indian Western Himalayas* (C. M. Neale & A. Maltese, Eds.; pp. 21–21). SPIE. <https://doi.org/10.1117/12.2636367>
- Jovanović, D., Govedarica, M., Sabo, F., Važić, R., & Popović, D. (2016). *Impact analysis of pansharpening Landsat ETM+, Landsat OLI, WorldView-2, and Ikonos images on vegetation indices* (K. Themistocleous, D. G. Hadjimitis, S. Michaelides, & G. Papadavid, Eds.; p. 968814). <https://doi.org/10.1117/12.2241543>
- Kaimuddin, M. I., Kusmana, C., & Setiawan, Y. (2023). Vegetation structure, biomass, and carbon of Mangrove Forests in Ambon Bay, Maluku, Indonesia. *Jurnal Pengelolaan Sumberdaya Alam Dan Lingkungan (Journal of Natural Resources and Environmental Management)*, 13(4), 710–722. <https://doi.org/10.29244/jpsl.13.4.710-722>
- Kang, M., & Katzfuss, M. (2023). Correlation-based sparse inverse Cholesky factorization for fast Gaussian-process inference. *Statistics and Computing*, 33(3), 56. <https://doi.org/10.1007/s11222-023-10231-5>
- Keskintürk, T., & Er, Ş. (2007). A genetic algorithm approach to determine stratum boundaries and sample sizes of each stratum in stratified sampling. *Computational Statistics & Data Analysis*, 52(1), 53–67. <https://doi.org/10.1016/j.csda.2007.03.026>
- Kluczek, M., Zagajewski, B., & Zwijacz-Kozica, T. (2023). Mountain Tree Species Mapping Using Sentinel-2, PlanetScope, and Airborne HySpex Hyperspectral Imagery. *Remote Sensing*, 15(3). Scopus. <https://doi.org/10.3390/rs15030844>
- Kotsiantis, S. B., Zaharakis, I. D., & Pintelas, P. E. (2006). Machine learning: A review of classification and combining techniques. *Artificial Intelligence Review*, 26(3), 159–190. <https://doi.org/10.1007/s10462-007-9052-3>
- Krishnan, M., & Dutta, D. (2017). A Study of Effectiveness of Principal Component Analysis on Different Data Sets. *2017 IEEE International Conference on Computational Intelligence and Computing Research (ICICR)*, 1–6. <https://doi.org/10.1109/ICICR.2017.8524329>
- Kuze, H., & Sumantyo, J. T. S. (2010). *Performance analyzing of high resolution pansharpening techniques: Increasing image quality for classification using supervised kernel support vector machine*. 260–268. Scopus. <https://www.scopus.com/inward/record.uri?eid=2-s2.0-79958713703&partnerID=40&md5=c2ed058cb88303665d14acbaae1babe>
- Labs, P. (2023). *PlanetScope: Daily global coverage*. <https://www.planet.com>
- Le, M. T., Tran, K. H., Dao, P. D., El-Askary, H., Ha, T. V., & Park, T. (2025). High spatial resolution crop type and land use land cover classification without labels: A framework using multi-temporal PlanetScope images and variational Bayesian Gaussian mixture model. *Science of Remote Sensing*, 12. Scopus. <https://doi.org/10.1016/j.srs.2025.100264>

- Leon, S. J., Björck, Å., & Gander, W. (2013). Gram-Schmidt orthogonalization: 100 years and more. *Numerical Linear Algebra with Applications*, 20(3), 492–532. <https://doi.org/10.1002/nla.1839>
- Liu, H. P., Wu, J. Q., Li, X. Y., Liu, Y. W., & Satybaldievna, C. D. (2025). TREE SPECIES IDENTIFICATION USING PRINCIPAL COMPONENT ANALYSIS FEATURES: AN ANALYSIS ON WHETHER NON-VEGETATION COMPONENTS SHOULD BE EXCLUDED. *Applied Ecology and Environmental Research*, 23(1), 1675–1686. https://doi.org/10.15666/aeer/2301_16751686
- Liu, J., Xue, X., Zuo, Q., & Ren, J. (2024). Classification of Hyperspectral-LiDAR Dual-View Data Using Hybrid Feature and Trusted Decision Fusion. *Remote Sensing*, 16(23), 4381. <https://doi.org/10.3390/rs16234381>
- Maciel Junior, I. C., Dallacort, R., Boechat, C. L., Teodoro, P. E., Teodoro, L. P. R., Rossi, F. S., Oliveira-Júnior, J. F. D., Della-Silva, J. L., Baio, F. H. R., & Lima, M. (2024). Maize Crop Detection through Geo-Object-Oriented Analysis Using Orbital Multi-Sensors on the Google Earth Engine Platform. *AgriEngineering*, 6(1), 491–508. Scopus. <https://doi.org/10.3390/agriengineering6010030>
- Mansaray, A. S., Dzialowski, A. R., Martin, M. E., Wagner, K. L., Gholizadeh, H., & Stoodley, S. H. (2021). Comparing PlanetScope to Landsat-8 and Sentinel-2 for Sensing Water Quality in Reservoirs in Agricultural Watersheds. *Remote Sensing*, 13(9), 1847. <https://doi.org/10.3390/rs13091847>
- Mateen, S., Nuthammachot, N., & Techato, K. (2024). Random forest and artificial neural network-based tsunami forests classification using data fusion of Sentinel-2 and Airbus Vision-1 satellites: A case study of Garhi Chandan, Pakistan. *Open Geosciences*, 16(1), 20220595. <https://doi.org/10.1515/geo-2022-0595>
- Mathur, A., & Foody, G. M. (2008). Crop classification by support vector machine with intelligently selected training data for an operational application. *International Journal of Remote Sensing*, 29(8), 2227–2240. <https://doi.org/10.1080/01431160701395203>
- Maurer, T. (2013). HOW TO PAN-SHARPEN IMAGES USING THE GRAM-SCHMIDT PAN-SHARPEN METHOD – A RECIPE. *ISPRS - International Archives of the Photogrammetry, Remote Sensing and Spatial Information Sciences*, XL-1/W1(May), 239–244. <https://doi.org/10.5194/isprsarchives-xl-1-w1-239-2013>
- Mikołajczyk, Ł., Hawryło, P., Netzel, P., Talaga, J., Zdunek, N., & Socha, J. (2025). Classification of Tree Species in Poland Using CNNs Tabular-to-Pseudo Image Approach Based on Sentinel-2 Annual Seasonality Data. *Forests*, 16(7). Scopus. <https://doi.org/10.3390/f16071039>
- Mohammadpour, P., & Viegas, C. (2022). Applications of Multi-Source and Multi-Sensor Data Fusion of Remote Sensing for Forest Species Mapping. In P. C. Pandey & P. Arellano (Eds.), *Advances in Remote Sensing for Forest Monitoring* (1st ed., pp. 255–287). Wiley. <https://doi.org/10.1002/9781119788157.ch12>
- Neyns, R., Efthymiadis, K., Libin, P., & Canters, F. (2024). Fusion of multi-temporal PlanetScope data and very high-resolution aerial imagery for urban tree species mapping. *Urban Forestry and Urban Greening*, 99. Scopus. <https://doi.org/10.1016/j.ufug.2024.128410>
- Niroumand-Jadidi, M., Legleiter, C. J., & Bovolo, F. (2022). River Bathymetry Retrieval from Landsat-9 Images Based on Neural Networks and Comparison to SuperDove and Sentinel-2. *IEEE Journal of Selected Topics in Applied Earth Observations and Remote Sensing*, 15, 5250–5260. Scopus. <https://doi.org/10.1109/JSTARS.2022.3187179>

- Njimi, H., Chehata, N., & Revers, F. (2024). Fusion of Dense Airborne LiDAR and Multispectral Sentinel-2 and Pleiades Satellite Imagery for Mapping Riparian Forest Species Biodiversity at Tree Level. *Sensors*, 24(6). Scopus. <https://doi.org/10.3390/s24061753>
- Njomaba, E., Ofori, J. N., Guuroh, R. T., Aikins, B. E., Nagbija, R. K., & Surový, P. (2024). Assessing Forest Species Diversity in Ghana's Tropical Forest Using PlanetScope Data. *Remote Sensing*, 16(3). Scopus. <https://doi.org/10.3390/rs16030463>
- Persson, M., Lindberg, E., & Reese, H. (2018). Tree Species Classification with Multi-Temporal Sentinel-2 Data. *Remote Sensing*, 10(11), 1794. <https://doi.org/10.3390/rs10111794>
- Planet Labs. (2023). *PlanetScope: Daily global coverage*. <https://www.planet.com>
- Purnamasari, E., Kamal, M., & Wicaksono, P. (2021). Comparison of vegetation indices for estimating above-ground mangrove carbon stocks using PlanetScope image. *Regional Studies in Marine Science*, 44, 101730.
- Rahmani, S., Strait, M., Merkurjev, D., Moeller, M., & Wittman, T. (2010). An Adaptive IHS Pan-Sharpening Method. *IEEE Geoscience and Remote Sensing Letters*, 7(4), 746–750. <https://doi.org/10.1109/LGRS.2010.2046715>
- Saboori, M., Asghar Torahi, A., & Reza Riyahi Bakhtyari, H. (2019). Combining multi-scale textural features from the panchromatic bands of high spatial resolution images with ANN and MLC classification algorithms to extract urban land uses. *International Journal of Remote Sensing*, 40(22), 8608–8634. <https://doi.org/10.1080/01431161.2019.1620371>
- Sechidis, K., Tsoumakas, G., & Vlahavas, I. (2011). On the Stratification of Multi-label Data. In D. Gunopulos, T. Hofmann, D. Malerba, & M. Vazirgiannis (Eds.), *Machine Learning and Knowledge Discovery in Databases* (Vol. 6913, pp. 145–158). Springer Berlin Heidelberg. https://doi.org/10.1007/978-3-642-23808-6_10
- Silva, A. G. P., Galvão, L. S., Ferreira Junior, L. G., Teles, N. M., Mesquita, V. V., & Haddad, I. (2024). Discrimination of Degraded Pastures in the Brazilian Cerrado Using the PlanetScope SuperDove Satellite Constellation. *Remote Sensing*, 16(13). Scopus. <https://doi.org/10.3390/rs16132256>
- Sule, S. D. (2020). Application of principal component analysis to remote sensing data for deforestation monitoring. In C. M. Neale & A. Maltese (Eds.), *Remote Sensing for Agriculture, Ecosystems, and Hydrology XXII* (p. 3). SPIE. <https://doi.org/10.1117/12.2573725>
- Swain, K. C., Singha, C., & Pradhan, B. (2024). Estimating Total Rice Biomass and Crop Yield at Field Scale Using PlanetScope Imagery Through Hybrid Machine Learning Models. *Earth Systems and Environment*, 8(4), 1713–1731. Scopus. <https://doi.org/10.1007/s41748-024-00481-2>
- Tsai, F., Lin, E. -K., & Yoshino, K. (2007). Spectrally segmented principal component analysis of hyperspectral imagery for mapping invasive plant species. *International Journal of Remote Sensing*, 28(5), 1023–1039. <https://doi.org/10.1080/01431160600887706>
- Uddin, M. P., Mamun, M. A., & Hossain, M. A. (2017). Improved Feature Extraction Using Segmented FPCA for Hyperspectral Image Classification. *2017 2nd International Conference on Electrical & Electronic Engineering (ICEEE)*, 1–4. <https://doi.org/10.1109/CEEE.2017.8412924>
- Ugm, F. K., & H, D. M. (2019). *Peta Kawasan Hutan Wanagama*. Fakultas Kehutanan UGM.
- Visentin, A., Prestwich, S., & Tarim, S. A. (2016). Robust Principal Component Analysis by Reverse Iterative Linear Programming. In P. Frasconi, N. Landwehr, G. Manco, & J.

- Vreeken (Eds.), *Machine Learning and Knowledge Discovery in Databases* (Vol. 9852, pp. 593–605). Springer International Publishing. https://doi.org/10.1007/978-3-319-46227-1_37
- Vivone, G., Simoes, M., Dalla Mura, M., Restaino, R., Bioucas-Dias, J. M., Licciardi, G. A., & Chanussot, J. (2015). Pansharpening Based on Semiblind Deconvolution. *IEEE Transactions on Geoscience and Remote Sensing*, 53(4), 1997–2010. <https://doi.org/10.1109/TGRS.2014.2351754>
- Wang, J., Song, G., Liddell, M., Morellato, P., Lee, C. K. F., Yang, D., Alberton, B., Detto, M., Ma, X., & Zhao, Y. (2023). An ecologically-constrained deep learning model for tropical leaf phenology monitoring using PlanetScope satellites. *Remote Sensing of Environment*, 286. Scopus. <https://doi.org/10.1016/j.rse.2022.113429>
- Xi, Y., Tian, J., Jiang, H., Tian, Q., Xiang, H., & Xu, N. (2022). Mapping tree species in natural and planted forests using Sentinel-2 images. *Remote Sensing Letters*, 13(6), 544–555. <https://doi.org/10.1080/2150704X.2022.2051636>
- Xi, Y., Zhang, W., Brandt, M., Tian, Q., & Fensholt, R. (2023). Mapping tree species diversity of temperate forests using multi-temporal Sentinel-1 and -2 imagery. *Science of Remote Sensing*, 8, 100094–100094. <https://doi.org/10.1016/j.srs.2023.100094>
- Xie, Y., Sha, Z., & Yu, M. (2008). Remote sensing imagery in vegetation mapping: A review. *Journal of Plant Ecology*, 1(1), 9–23. <https://doi.org/10.1093/jpe/rtm005>
- Xu, K., Han, H., Wang, S., Zhao, P., Geng, J., Jiang, H., & Ding, A. (2025). TS2GNet: A temporal–spatial–spectral multidomain guided network for classifying hyperspectral tree species using multiseason satellite imagery. *International Journal of Applied Earth Observation and Geoinformation*, 142, 104715. <https://doi.org/10.1016/j.jag.2025.104715>
- Yu, W., Zhao, P., Xu, K., Zhao, Y., Shen, P., & Ma, J. (2022). Evaluation of red-edge features for identifying subtropical tree species based on Sentinel-2 and Gaofen-6 time series. *International Journal of Remote Sensing*, 43(8), 3003–3027. Scopus. <https://doi.org/10.1080/01431161.2022.2079018>
- Zhang, Y., Wang, H., Mao, R., Chen, B., & Jiang, M. (2025). A novel data fusion strategy of LC-MS and NMR technologies using random forest model for emodin hepatotoxic metabolomics research. *Journal of Pharmaceutical and Biomedical Analysis*, 264, 116990. <https://doi.org/10.1016/j.jpba.2025.116990>